Chemosphere 147 (2016) 60–66

Contents lists available at ScienceDirect

Chemosphere

journal homepage: www.elsevier.com/locate/chemosphere

Ultrafine particles derived from mineral processing: A case study of the Pb–Zn sulfide ore with emphasis on lead-bearing colloids

Yuri Mikhlin [a, *], Sergey Vorobyev [a, b], Alexander Romanchenko [a], Sergey Karasev [a], Anton Karacharov [a], Sergey Zharkov [b, c]

[a] Institute of Chemistry and Chemical Technology of the Siberian Branch of the Russian Academy of Sciences, Akademgorodok, 50/24, Krasnoyarsk, 660036, Russia
[b] Siberian Federal University, Svobodny pr. 79, Krasnoyarsk, 660041, Russia
[c] Kirensky Institute of Physics of the Siberian Branch of the Russian Academy of Sciences, Akademgorodok 50/38, Krasnoyarsk, 660036, Russia

HIGHLIGHTS

- The yield of (sub)micrometer particles of the ground ore was determined.
- Aqueous supernatant from the ore contains colloidal aggregates depleted in Si, Al, Fe.
- Colloidal PbS nanoparticles are associated with lead sulfate and thiosulfate.
- Metal sulfide colloids are more stable than the mineral aggregates.
- PbS nanoparticles can be well mobilize from ore sediments with water.

ARTICLE INFO

Article history:
Received 11 October 2015
Received in revised form
22 December 2015
Accepted 23 December 2015
Available online 4 January 2016

Handling Editor: Martine Leermakers

Keywords:
Lead-zinc ore
Lead sulfide
Ultrafine particles
Aquatic nanoparticles

ABSTRACT

Although mining and mineral processing industry is a vast source of heavy metal pollutants, the formation and behavior of micrometer- and nanometer-sized particles and their aqueous colloids entered the environment from the technological media has received insufficient attention to date. Here, the yield and characteristics of ultrafine mineral entities produced by routine grinding of the Pb–Zn sulfide ore (Gorevskoe ore deposit, Russia) were studied using laser diffraction analysis (LDA), dynamic light scattering (DLS) and zeta potential measurement, microscopy, X-ray photoelectron spectroscopy, with most attention given to toxic lead species. It was revealed, in particular, that the fraction of particles less that 1 μm in the ground ore typical reaches 0.4 vol. %. The aquatic particles in supernatants were micrometer size aggregates with increased content of zinc, sulfur, calcium as compared with the bulk ore concentrations. The hydrodynamic diameter of the colloidal species decreased with time, with their zeta potentials remaining about −12 mV. The colloids produced from galena were composed of 20–50 nm PbS nanoparticles associated with lead sulfate and thiosulfate, while the surface oxidation products at precipitated galena were largely lead oxyhydroxides. The size and zeta potential of the lead-bearing colloids decreased with time down to about 100 nm and from −15 mV to −30 mV, respectively. And, conversely, lead sulfide nanoparticles were mobilized before the aggregates during redispersion of the precipitates in fresh portions of water. The potential environmental impact of the metal-bearing colloids, which is due to the large-scale production and relative stability, is discussed.

1. Introduction

Sulfide minerals of heavy metals, including lead and zinc, are the main source of these metals. The metal values are commonly separated from gangue minerals by froth flotation of particles about 40 μm or coarser produced by milling the ore, with smaller mineral particles inevitably emerging as a result of over-grinding and secondary processes. The recovery of fine, below approximately 20 μm, metal sulfide particles decreases (Trahar, 1981; Cullinan et al., 1999; Feng and Aldrich, 1999; Johnson, 2006); oxidized fines and slimes have a detrimental effect on flotation performance (Bandini et al.,

* Corresponding author.
E-mail address: yumikh@icct.ru (Y. Mikhlin).

http://dx.doi.org/10.1016/j.chemosphere.2015.12.096
0045-6535/

2001; Grano, 2009; Peng and Grano, 2010). The ultrafine particles then enter tailing dumps, waste waters, mine drainage and natural drainage, polluting soils, surface- and ground waters (Hudson-Edwards, 2003; Hu et al., 2008; Boyd, 2010; Wang et al., 2014). Metal sulfide nanoparticles arise also in the nature (Rozan et al., 2000, 2003; Luther and Rickard, 2005; Wigginton et al., 2007; Hochella et al., 2008; Hotze et al., 2010; Wang, 2014), mobilizing the metals in quantities which can be higher than solubility of cations in hydrothermal fluids and surface waters (Gammons and Frandsen, 2001; Hofacker et al., 2013; Plathe et al., 2013). Just as an example, Weber et al. (2009) have reported that biota-assisted formation of colloidal Cu, Cd and Pb sulfides increased the contaminant mobilization to 8, 4 and 22 times, respectively. Very fine metal sulfide can emerge as their precipitation is used to remove heavy metals from water (Banfalvi, 2006; Castillo et al., 2012). Increasing attention is paid now to the environmental fate of engineered nanomaterials, including water-soluble quantum dots of metal sulfides and oxides which are of interest for the emerging nanotechnology applications (Auffan et al., 2010; Liu et al., 2009; Hou et al., 2013; Cornelis et al., 2014; Garner and Keller, 2014). The volume of ultrafine lead and other heavy-metal bearing solids originating from mineral processing should be much larger than from nanomaterials, shooting range soils (Cao et al., 2003; Hardison et al., 2004; Lewis et al., 2010), or other industries, but data on their yield, granulometric and chemical composition, colloidal stability and other properties are very poor till now, despite this information can be important for geochemistry, environmental science, water treatment, flotation practice (Crane and Scott, 2012; Fu and Wang, 2011; Hashim et al., 2011; Wang et al., 2014; Keim and Markl, 2015); reliable techniques for such studies remain a challenge too (Zirkler et al., 2012).

The aim of this work was to gain insights into the formation and characteristics of ultrafine mineral particles in case of conventional, typical for flotation, milling of a Pb–Zn sulfide ore from Gorevskoe deposit (Siberia, Russia), pure galena, PbS, and, in less extent, sphalerite, ZnS. A combination of electron and scanning probe microscopy, laser diffraction and dynamic light scattering, zeta potential measurement, X-ray photoelectron spectroscopy (XPS) was utilized to examine the yield of the fines (approaching several kilograms per ton), and the morphology, composition and colloidal stability of the aquatic particles. Special attention been given to lead species as the most dangerous for biota and human health (Shahid et al., 2012; Truong et al., 2010; Hou et al., 2013), particularly as there is considerable risk of water contamination from the Gorevskoe mining and milling facilities located near the large Angara River. The experimental data are discussed in terms of environmental behavior of the colloidal species.

2. Experimental

2.1. Materials

Pb–Zn sulfide ore from Gorevskoe deposit (Krasnoyarsk Territory, Russia) had an average elemental composition, wt. %: Pb 6.4, Zn 2.2, Fe 19.7, S 4.3, Si 18.0, Al 2.6, Ca 3.2, Mg 1.4, O 42.2. The main sulfide minerals are galena (PbS), pyrrhotite (Fe_7S_8), sphalerite (ZnS), and gangue minerals are presented by quartz, chlorites, siderite ($FeCO_3$), dolomite ($(Mg,Ca)CO_3$), calcite ($CaCO_3$), and some others. Ore samples crushed down to 5 mm were ground in a steel ball mill to 80% finer than 74 μm at solid/water/balls weight ratio of 1:0.4:9 (60 min); dry milling was also performed under analogous conditions. A portion of the ground ore was sieved to fractions after air drying. Galena and sphalerite minerals without visible inclusions of foreign phases were ground to −74 μm (80%) in the same way.

For examination of the slurries and colloidal particles, the ground samples were dispersed (10 wt. %) in doubly distilled water and agitated in a glass beaker for 5 min, and then left to precipitate at room temperature (22 ± 1 °C). After a predetermined time, portions of supernatant taken by a pipette from about 1 cm below the solution surface were collected for characterization. pH value was monitored through the experiment but no pH corrections were made; typically, pH was 7.3 ± 0.4 in the ore slurries and 6.0 ± 0.2 in the PbS slurries.

2.2. Electron microscopy and scanning probe microscopy

The ground and dried samples were characterized with scanning electron microscopy (SEM), backscattered electron imaging microanalysis (SEM–BSE), and energy dispersive X-ray spectroscopy (EDX) using a Hitachi TM 3000 instrument operated at acceleration voltage of 15 kV, equipped with a Bruker Quantax 70 EDX analyzer. Transmission electron microscopy studies were performed with a JEM-2100 microscope (JEOL) operated at 200 kV. Samples were prepared by placing a supernatant droplet taken from a slurry directly before the measurement on a carbon coated copper grid and allowing water to evaporate at room temperature.

Tapping-mode atomic force microscopy (AFM) investigations were conducted in air (the relative humidity was about 60%) applying a multimode Solver P47 device equipped with a 14 mm scanner (NT-MDT, Russia). Silicon cantilevers with a typical force constant of 5 N m^{-1} (resonant frequencies of about 150 kHz) were employed. Samples were prepared by drying a supernatant drop on highly-oriented pyrolytic graphite (HOPG).

2.3. Laser diffraction, dynamic light scattering and zeta-potential measurement

Particle size distributions were determined in water suspensions using laser diffraction analysis with Horiba LA-300 instrument and dynamic light scattering (DLS) with Zetasizer Nano ZS spectrometer (Malvern Instruments Ltd). The volume fractions of particles were calculated from the frequency distributions, assuming the particles spherical, using the software implemented in the instruments. Zeta potential distributions both of precipitates and aquatic colloid particles in supernatants were measured with Zetasizer Nano ZS instrument in a folded polycarbonate cell with Pd electrodes at 20 °C; no additional grinding was applied and no electrolyte was added.

2.4. X-ray photoelectron spectroscopy (XPS)

X-ray photoelectron spectra were collected with a SPECS instrument equipped with a PHOIBOS 150 MCD 9 hemispherical analyzer at electron take-off angle 90°. The Mg Kα line (1253.6 eV) of a dual anode X-ray source or monochromatized Al Kα line (1486.6 eV) were used for excitation. The pressure in an analytical chamber was in the range of 10^{-9} mBar. The binding energies were corrected using the C 1s reference (285.0 eV) from aliphatic carbon; a low-energy electron flood gun was employed to eliminate inhomogeneous electrostatic charging of the samples. The spectra were fitted using Gaussian–Lorentzian peak profiles after Shirley background subtraction with CasaXPS software.

3. Results

3.1. SEM and laser diffraction analysis

Typical micrographs of the Pb–Zn ore and galena after the milling are presented in Fig. 1, where galena crystals are light-

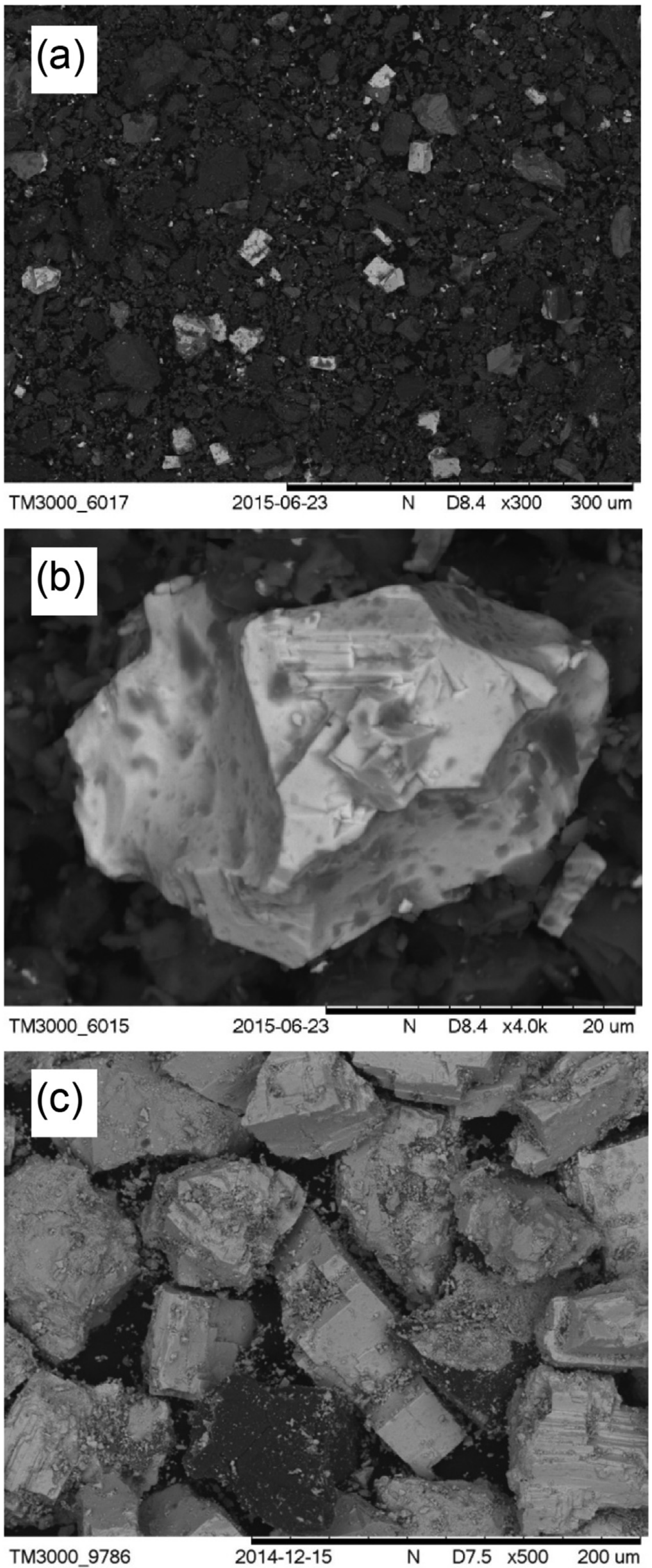

Fig. 1. Representative SEM micrographs of ground (a, b) Pb–Zn ore and (c) galena.

colored; more data including the elemental distribution map can be seen in Supplementary Information. One can see that there exist a considerable number of fine particles of several micrometer in size and smaller both in the ground ore and galena.

Fig. 2 a, b show the granulometries of the Pb–Zn ore and galena ground to less than 74 μm (80%), which was determined using laser diffraction analysis; the composition of sieved fractions is also present. The size frequency distributions for the ore have the main maximum at about 20 μm and minor ones at about 2 μm and 0.25 μm; the fines are largely related with the fraction of −44 μm. The contents of particles smaller than 1 μm calculated from these data approach 0.4 vol. % and 0.15 vol. % in the wet and dry milled ore, respectively (Table 1). Pure galena milled under the same conditions (Fig 2 c) exhibits the maximum of the size distribution at about 25 μm and, for the dry milled samples, a pronounced second peak at about 90 μm; the yield of submicrometer particles is lower than for the ore (Fig. 2c).

3.2. *Colloidal particles (TEM, AFM and dynamic light scattering and zeta-potential)*

An example of aquatic particles occurring in the supernatants above the ore sediment can be seen in TEM images (Fig. 3). There exist mainly micrometer-size aggregates of different particles including nanoparticles of PbS and ZnS; EDX analysis (not in Figures) performed in various spots revealed very diverse composition, including Si, Fe, Al, Mg, Pb, Zn, S and other elements. It is interesting that mineral nanocrystals are often coated with amorphous matter, as an example, one can see a layered chlorite (interplanar distances of about 0.49 nm and 0.25 nm) and a gypsum nanoparticle (0.224 nm) in HRTEM. The TEM micrograph of the colloidal particles produced from galena (Fig. 3b) also shows dense 10–100 nm PbS particles aggregated with less contrasted and possibly amorphous particulate matter composed of products of galena oxidation (see also De Giudici and Zuddas, 2001).

AFM images of supernatant droplets dried at HOPG (see Supplementary Information, Fig. S3) revealed irregular submicrometer islands consisting from nanoparticles with the height less than 50 nm. The data suggest that the species have poor adhesion to the hydrophobic HOPG surface, probably, because of the hydrophilic oxidized coating on the PbS particles. Interestingly, addition of potassium n-butyl xanthate, that is a common flotation collector, makes the particles adhered to and uniformly distributed over the HOPG as result of the particle hydrophobization.

The dimensions of suspended mineral particles smaller than 10 μm were evaluated using DLS (Fig. 4). The hydrodynamic diameter distribution for the particles in the supernatant formed after 10 min precipitation of freshly prepared slurries of the ground Pb–Zn ore typically had two maxima or shoulder at 1–2 μm and about 5 μm. The distributions somewhat differ for various fractions, the milling mode (wet or dry) and depend upon the decantation time; naturally, the total amount and the average size of the colloids decreases with time due to precipitation of larger particles. The particles having the hydrodynamic diameter about 1.3 μm may be relatively stable and dominates the hydrosols up to several hours. Zeta-potential of the particles is negative, showing one peak with rather low magnitude of approximately −12 mV at the pH ~7.5 and almost independent on time. This suggests effectively uniform surface composition of the particles and explains their rather low aggregative stability.

The hydrodynamic diameters of galena particles behave similarly, but the negative zeta potential magnitudes were larger and shifted to more negative values with time. This can be rationalized in terms of preferential coagulation and precipitation of particles with less negative zeta-potential, probably more oxidized ones, that is, products of lead sulfide oxidation (lead sulfate, lead oxyhydroxides, elemental sulfur and so on), both separated and immobilized at PbS surfaces (see Fig. 3b), while less oxidized PbS with more negative potential stay in the aqueous phase (see, for instance, Peng and Grano, 2010, and references therein).

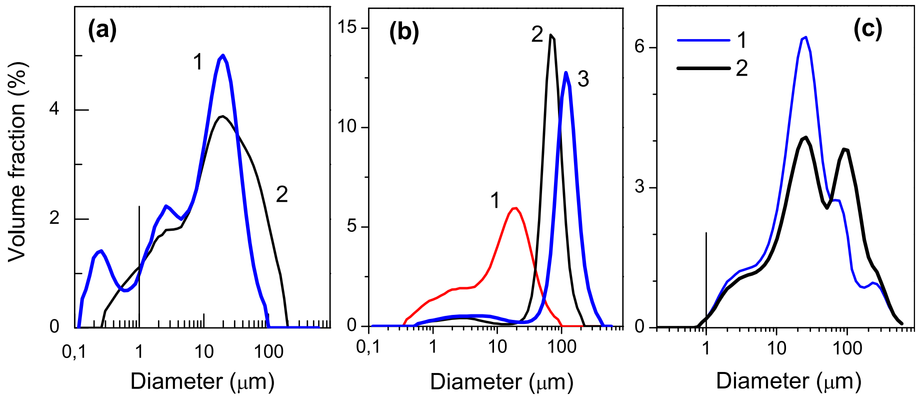

Fig. 2. Particle size distributions of (a) ground Pb–Zn ore (1 – wet, 2 – dry milling) and (b) the sieved fractions after the wet milling (1 – <44 μm, 2–44–76 μm, 3–76 – 125 μm); (c) PbS milled for 20 min (1 – wet, 2 – dry) determined using laser diffraction analysis.

Table 1
The yield of fine particle fractions (vol. %) of the Pb–Zn ore and galena (PbS) ground to −74 μm (80%) as calculated from laser diffraction analysis data.

Sample	0 – 1 μm	0 – 5 μm	0 – 10 μm
dry milled Pb–Zn ore	0.15	1.9	5.2
wet milled Pb–Zn ore	0.39	4.3	10.7
dry milled galena	0.04	0.89	2.6
wet milled galena	0.03	1.2	3.7

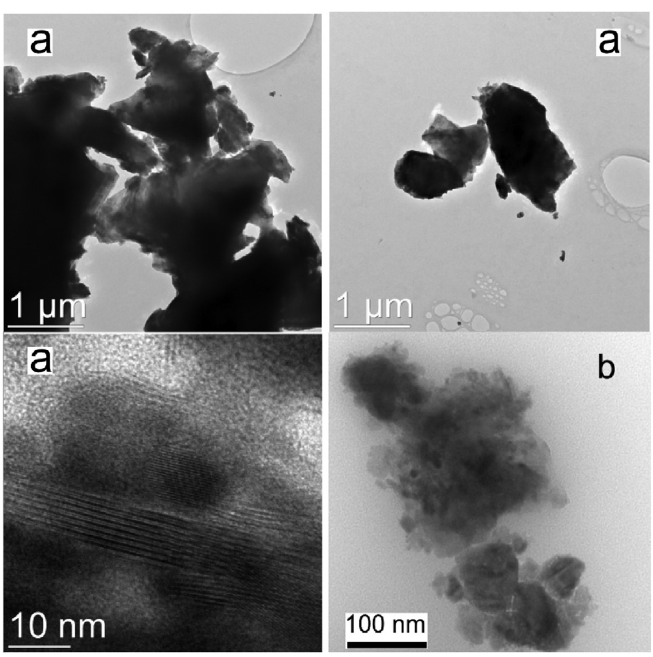

Fig. 3. TEM images of particles from the supernatant above (a) Pb–Zn ore and (b) galena after 10 min sedimentation.

We also examined colloidal particles produced by re-dispersion of the ground galena in fresh portions of water (Fig. 5). During the washing out, which takes place in the environment, for example, due to flooding of mines and concentrating mill tailings, smaller lead-bearing particles with the average hydrodynamic diameter of 100–200 nm and zeta potential more negative than −20 mV arise in the first wash cycle. The zeta-potentials decreases in absolute value to about −12 mV; the average size of nanoparticles gradually increases and then a fraction of about 1 μm particles emerges and

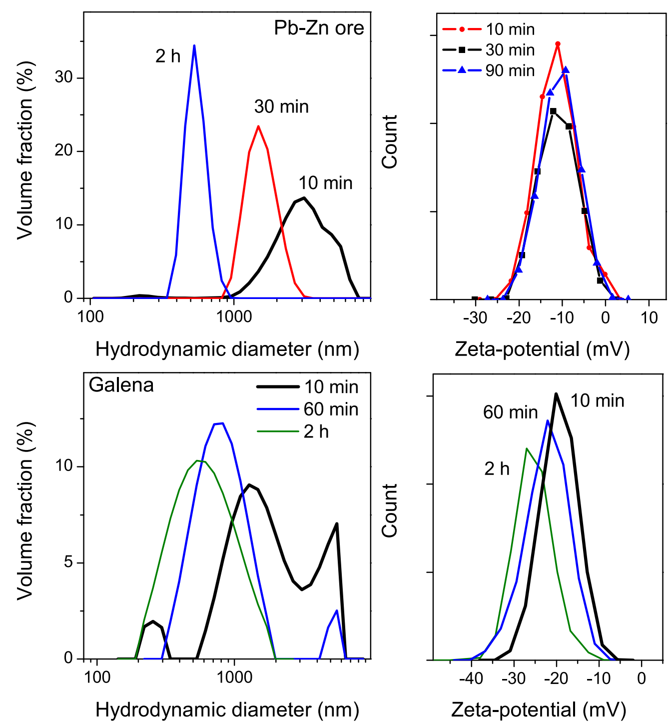

Fig. 4. Hydrodynamic diameter and zeta-potential distributions in supernatant above precipitated Pb–Zn ore and galena (fractions −44 μm) for various sedimentation times.

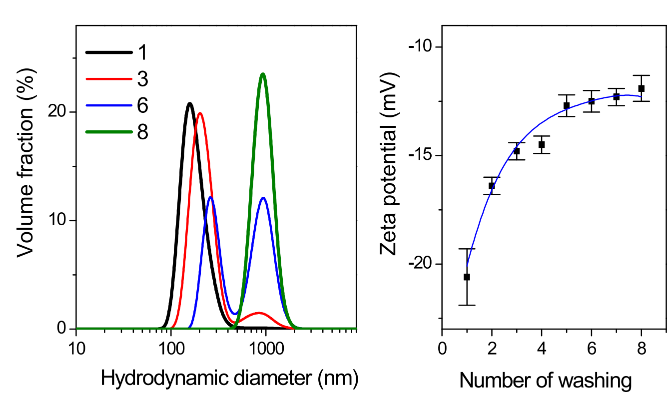

Fig. 5. Hydrodynamic diameter and zeta-potential distributions in supernatant above ground galena washed with fresh portions of water; the curves in the left panel are marked with the number of wash steps.

grows in subsequent wash steps with fresh portions of water. Therefore, less oxidized PbS nanoparticles used to mobilize first, and solubilization of oxidized aggregated entities is more difficult, despite their hydrophilic surfaces.

Attempts to separate and characterize fine particles by using filtration, centrifugation, and sedimentation techniques were also undertaken, however, the results were ambiguous. Filtration of supernatants, not to mention the slurries, with a 450 nm pore filter produced filtrates, in which no colloidal particles were found with DLS. This method, consequently, should not be used in the granulometric analysis of such materials. The composition of supernatants prepared by means of centrifugation depended upon the rotation frequency and time; typically, the average size of colloidal particles in supernatant decreased to about 100 nm.

3.3. X-ray photoelectron spectroscopy

The elemental surface concentrations found by XPS analysis (Supplementary Information Table S1) mainly agree with the net contents in the ore; the results show that the sieved fraction −44 μm was slightly enriched with zinc relative to lead, iron and sulfur, possibly because fine particles galena and pyrrhotite were more oxidized. Carbon was largely due to surface hydrocarbon contaminations and, in case of supernatant droplets dried on HOPG, signals of the supporting graphite, and its content was disregarded. The narrow C 1s scans (not in Figures) revealed, nevertheless, that carbonate component approached about 10% of carbon (and 3–4 at % total) in the ore almost disappeared in the supernatants. The supernatants also had reduced relative contents of Si, Al, and Fe and increased ones of S, Zn, Ca, Mg, K. The proportions of Ca, Mg and Zn steadily grew with the time of sedimentation, those of Si, Al and Pb gradually decreased, while S and Fe stayed almost constant over several hours.

The high-resolution Pb 4f spectra (Fig. 6) can be fitted using two doublets from PbS and lead bonded to oxygen in thiosulfate and sulfate and (hydro)oxide with Pb $4f_{7/2}$ maxima centered at 137.6 eV and about 138.5 eV, respectively. The share of Pb atoms bonded to S was about 55% for the ground ore and 65–80% for the pure galena milled under similar conditions, indicating that the oxidation of PbS is facilitated by other minerals upon milling, probably, owing to galvanic effects and direct oxidation by ferric ions.

The S 2p spectra of the ore have contributions from the oxidized surfaces of PbS, pyrrhotite, sphalerite which are difficult to interpret in detail. The intensities of sulfidic species (including di- and polysulfide) were notably larger than those of S–O species (sulfate and thiosulfate), especially for ground galena (Fig. 6), suggesting that the oxidized surface species at rather big galena particles are mainly lead oxide and hydroxide. However, lead sulfate and thiosulfate, which prevailed in the supernatants both above the ore and galena sediments, seem to be the main surface product at small oxidized mineral particles, although these substances could form their own nanoparticles. In contrast, colloidal sphalerite prepared by milling the pure mineral was much less oxidized and bore low oxysulfur compounds (not in Figures), although enhanced amounts of di- and polysulfide species indicated notably metal-deficient surface of the submicrometer particles.

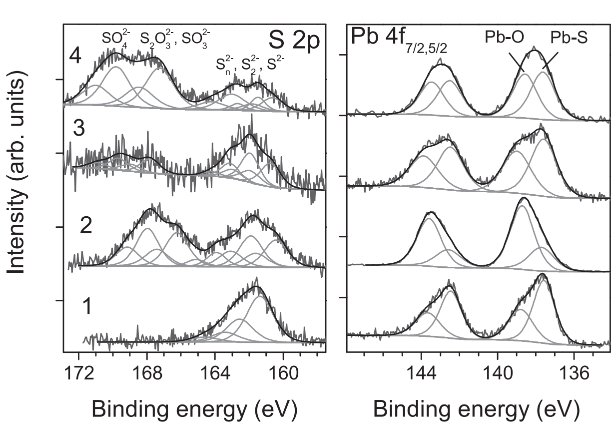

Fig. 6. X-ray photoelectron S 2p and Pb 4f spectra from (1, 3) precipitate and (2, 4) supernatant droplet for (1, 2) galena and (3, 4) Pb–Zn ore milled and dispersed in water after 10 min sedimentation.

4. Discussion

The Pb–Zn ore of the Gorevskoe deposit does not contain remarkable quantities of ultrafine minerals and is not inclined to overgrinding; nevertheless, the conventional milling procedure produces several kilograms of ultrafine, a micrometer-size and smaller, solid particles per ton of the ground ore. Gangue minerals (silicates and aluminosilicates, carbonates), and products of the metal sulfide oxidation, first of all ferric oxyhydroxides are commonly believed to be the principal substances forming fines and slimes in the mineral processing (Bandini et al., 2001; Peng and Grano, 2010). The yield of ultrafine particles upon milling galena and sphalerite is several times lower, but their contents in colloidal solutions are enhanced relative to the gangue minerals and iron oxyhydroxides. The depletion of the supernatants with Si-, Al- and Fe-bearing compounds can be explained mainly by their rapid aggregation and precipitation due to rather low surface charge (Fig. 4) and so low stability of their hydrosols and the deposition (immobilization) of these species at larger mineral particles. In turn, stable colloids could accumulate in the slurries and recycled water and enter the waste waters and the environment.

The lead-bearing colloids are typically composed of lead sulfide nanoparticles of 20–50 nm in size associated with the oxidation products, mainly lead sulfate and thiosulfate, and possibly some species akin to ferric oxyhydroxides, which promote the formation of Pb-bearing aggregates as large as several micrometers, tending to coagulation. As the sedimentation proceeds, less oxidized PbS particles with more negative zeta-potentials remain in the aqueous media. Their precipitation may be caused by gradual chemical oxidation of PbS surfaces that is faster in acidic media and slower at higher pHs (Cama et al., 2005; De Giudici et al., 2005; Mikhlin et al., 2006; Liu et al., 2008, 2009; Keim and and Markl, 2015). Lead sulfide oxidation may be suppressed, and then the mobility of metal-bearing colloids increased, by sulfate-reducing bacteria (Weber et al., 2009; Castillo et al., 2012) and by some abiotic reactions, including the interaction with surfactants originating from the technological media, particularly flotation reagents akin xanthates and others, and the environment (Liu et al., 2008, 2009; Hofacker et al., 2013; Mudunkotuwa and Grassian, 2011). Sphalerite is more resistant to oxidation and so its colloids are more stable, but their environmental role may be less important since zinc is substituted by copper and lead (Tang et al., 2002; Weber et al., 2009; Castillo et al., 2012; Deonarine et al., 2011); furthermore, the content of zinc in the Gorevskoe ore deposit is four times lower than lead. The reverse process of extraction of lead from the tailings via their contact with waters will result in the mobilization of colloidal PbS nanoparticles in the first step; oxidized aggregates are less mobile and can be washed out in the next cycles of the watering, although their stability against precipitation is expected to be low. The above experiments also showed that aquatic particles can be lost during analysis when inappropriate procedures, e.g. filtration of supernatants, are applied (see also Zirkler et al., 2012 for more examples). So, the role of aquatic micrometer aggregates

analytical TEM analyses after nanoparticle isolation and density separation. Geochim. Cosmochim. Acta 102, 213–225.

Rozan, T.F., Lassman, M.E., Ridge, D.P., Luther III, G.W., 2000. Evidence for iron, copper and zinc complexation as multinuclear sulphide clusters in oxic rivers. Nature 406, 879–882.

Rozan, T.F., Luther III, G.W., Ridge, D., Robinson, S., 2003. Determination of Pb complexation in oxic and sulfidic waters using pseudovoltammetry. Environ. Sci. Technol. 37, 3845–3852.

Shahid, M., Pinelli, E., Dumat, C., 2012. Review of Pb availability and toxicity to plants in relation with metal speciation; role of synthetic and natural organic ligands. J. Hazard. Mat. 219–220, 1–12. http://dx.doi.org/10.1016/j.jhazmat.2012.01.060.

Tang, D., Warnken, K.W., Santschi, P.H., 2002. Distribution and partitioning of trace metals (Cd, Cu, Ni, Pb, Zn) in Galveston bay waters. Mar. Chem. 78, 29–45.

Trahar, W.J., 1981. A rational interpretation of the role of particle size in flotation. Int. J. Min. Process 8, 289–327. http://dx.doi.org/10.1016/0301-7516(81)90019-3.

Truong, L., Moody, I.S., Stankus, D.P., Nason, J.A., Lonergan, M.C., Tanguay, R.L., 2010. Differential stability of lead sulfide nanoparticles influences biological responses in embryonic zebrafish. Arch. Toxicol. 85, 787–798. http://dx.doi.org/10.1007/s00204-010-0627-4.

Wang, Y., 2014. Nanogeochemistry: nanostructures, emergent properties and their control on geochemical reactions and mass transfers. Chem. Geol. 378–379, 1–23. http://dx.doi.org/10.1016/j.chemgeo.2014.04.007.

Wang, C., Harbottle, D., Liu, Q., Xu, Z., 2014. Current state of fine mineral tailings treatment: a critical review on theory and practice. Min. Eng. 58, 113–131. http://dx.doi.org/10.1016/j.mineng.2014.01.018.

Weber, F.-A., Voegelin, A., Kaegi, R., Kretzschmar, R., 2009. Contaminant mobilization by metallic copper and metal sulphide colloids in flooded soil. Nat. Geosci. 2, 267–271.

Wigginton, N.S., Haus, K.L., Hochella Jr., M.F., 2007. Aquatic environmental nanoparticles. J. Environ. Monit. 9, 1306–1316.

Zirkler, D., Lang, F., Kaupenjohann, M., 2012. "Lost in filtration" — the separation of soil colloids from larger particles. Colloids Surf. A 399, 35–40. http://dx.doi.org/10.1016/j.colsurfa.2012.02.021.